PNAS RESEARCH ARTICLE | PHYSIOLOGY

Asymmetric development and function of paired sperm-storage organs in *Drosophila melanogaster*

Dawn S. Chen[a,1,2], Kianairy Marrero[b,1], Javier Arturo Sanchez-Lopez[c,1], Michael Belenky[c], Jonathon M. Thomalla[a], Norene A. Buehner[a], Ido Apel[c], Yarin Levi[c], Yassi Hafezi[a], Shuran Wang[a], Andrew G. Clark[a,3], Yael Heifetz[c,3], Mark L. Siegal[b,3], and Mariana F. Wolfner[a,3]

Affiliations are included on p. 9.

Contributed by Mariana F. Wolfner; received May 29, 2025; accepted July 17, 2025; reviewed by John M. Belote and John P. Masly

Paired structures often have similar forms and functions, but the processes underlying their formation can differ. They may originate from a common source or from parallel sources, or arise from distinct precursors that follow separate developmental pathways, ultimately converging on comparable structures and roles. When asymmetries emerge and persist through development, members of the pair can specialize in ways that might increase fitness. Here, we report that the *Drosophila melanogaster* female's pair of spermathecae, which appear similar and have the common role of sperm storage, derive from different developmental compartments defined by expression of lineage-tracing markers corresponding, respectively, to the key patterning genes *engrailed* and *wingless*. We further find that the two spermathecae show significant differences in size, secretory activity, and calcium levels and, perhaps as a consequence, sperm retention dynamics. These results open broad avenues for understanding how developmental, physiological, and behavioral asymmetries arise and impact reproductive success.

spermatheca | sperm storage | paired organs | compartments | calcium

Paired organs, found in a wide variety of animals, play crucial roles in physiologic processes. These organs often exhibit symmetry in both structure and function, but in some cases they have evolved subtle or pronounced differences that allow for specialization. Such differences can benefit the organism by enabling the organs in the pair to perform complementary or entirely distinct functions. Understanding the interplay between symmetry and asymmetry in paired organs provides key insights into the adaptive pressures that shape organ development and function.

A classic example of paired organs are the kidneys in vertebrates, which maintain near-perfect symmetry in structure and function. Their primary roles in filtration and osmoregulation are evenly divided, with both kidneys working together to cleanse the blood and maintain homeostasis (1). However, other paired systems exhibit varying degrees of asymmetry. In certain fish species, such as the flounder, one eye migrates to the opposite side of the body during development, leading to the lateralized placement of both eyes on one side of the head. This adaptation enhances the fish's ability to camouflage itself on the ocean floor while retaining binocular vision (2). Another example can be found in male canaries, whose vocal pathways are bilaterally asymmetric, with the right and left pathways being responsible for different aspects of their song (3). Additionally, male fiddler crabs display claw asymmetry associated with their claw-waving behavior (4). Asymmetry may also be purely anatomic, without any functional effect, such as in human lungs, where the left lung possesses an indentation called the cardiac notch to accommodate the adjacent heart (5).

In reproductive systems, paired organs can display pronounced functional asymmetry, particularly in species where one organ of the pair becomes the dominant or exclusive contributor to reproductive processes. For example, in various snake species, the paired male reproductive organs, or hemipenes, are often morphologically distinct, with one side typically being larger or more frequently used during mating (6). The asymmetry in the hemipenes, an adaptation to the snakes' coiling bodies, allows for versatility during copulation depending on the male's orientation relative to its mate. Another example is in birds, which typically have two ovaries, but most species use only one, with the right ovary often regressing during development (7). The adaptive value of this functional reduction is not certain but might be related to energy conservation during flight. In humans, ovarian asymmetry is less pronounced but is present: the right one demonstrates higher ovulation frequency, thought to be a side effect of differences in vascularization of the right and left sides of the pelvic area (8).

Significance

Asymmetry of paired organs has been observed across animal species, from the claws of crustaceans to the reproductive organs of snakes. Females of the fly *Drosophila melanogaster* have a pair of organs called spermathecae that store sperm after mating. We show that the *D. melanogaster* spermathecae, which appear similar to each other, actually differ in their developmental origins, sperm retention dynamics, and some physiological parameters. Our findings establish this major laboratory organism as a model for the mechanisms and consequences of asymmetric sperm storage, a phenomenon that contributes to reproductive success in insects of agricultural and public-health importance.

Author contributions: D.S.C., K.M., J.A.S.-L., J.M.T., Y. Hafezi, A.G.C., Y. Heifetz, M.L.S., and M.F.W. designed research; D.S.C., K.M., J.A.S.-L., M.B., J.M.T., N.A.B., I.A., Y. Hafezi, and S.W. performed research; D.S.C., J.A.S.-L., J.M.T., I.A., Y.L., A.G.C., Y. Heifetz, M.L.S., and M.F.W. analyzed data; and D.S.C., M.B., J.M.T., A.G.C., Y. Heifetz, M.L.S., and M.F.W. wrote the paper.

Reviewers: J.M.B., Syracuse University; and J.P.M., University of Southern California.

Competing interest statement: Both reviewers and authors Heifetz, Siegal, and Wolfner were part of a broad consortium that published a standardized nomenclature/atlas of *Drosophila melanogaster* terminalia in 2022. There was no direct collaboration among the present reviewers and authors on that nomenclature paper.

[1]D.S.C., K.M., and J.A.S.-L. contributed equally to this work.

[2]Present address: Department of Biology, University of Pennsylvania, Philadelphia, PA 19104.

[3]To whom correspondence may be addressed. Email: ac347@cornell.edu, yael.heifetz@mail.huji.ac.il, mark.siegal@nyu.edu, or mfw5@cornell.edu.

This article contains supporting information online at https://www.pnas.org/lookup/suppl/doi:10.1073/pnas.2512096122/-/DCSupplemental.

Published August 19, 2025.

The spermathecae of *Drosophila melanogaster* females are paired organs that are important for fertility. These organs serve as long-term sperm-storage reservoirs and endocrine glands (9). The two spermathecae appear grossly identical, are similarly dependent for their development on genes such as *lozenge* (*lz*) (10, 11), *Hr39* (12), and *Notch* (13), and show similar expression of genes such as *Send1* and *Send2* (14). Nonetheless, there are reasons to suspect that they might differ. For example, *Aedes aegypti* and other Culicine mosquitoes have three spermathecae: one large medial one and two small lateral ones (15). The yellow dung fly *Scathophaga stercoraria* has three spermathecae as well—a doublet on one side and a singlet on the other. Moreover, dung fly spermathecae have been reported to differ in function: the long sperm from larger males are more likely to be stored in the singlet (16). Likewise, there is asymmetry of sperm storage in the spermathecae of the Mediterranean fruit fly *Ceratitis capitata*, depending on the condition of the male. *C. capitata* females have two spermathecae, with a greater differential between the two in the number of sperm stored when the total number of sperm stored is lower, such as following matings with less well-fed males (17). Last, symmetry of spermathecal sperm storage appears to be sensitive to genetic or environmental perturbation in *D. melanogaster*. Specifically, a significant asymmetry in spermathecal sperm storage has been demonstrated in *Gld*-null *D. melanogaster* females (18), suggesting an innate difference in glucose dehydrogenase activity (or its requirement) between the spermathecae. In another example, a substantial number of females with sperm in only one spermatheca is seen in mates of males raised at warm temperatures (19), suggesting an innate difference in heat tolerance. Together, these findings point to a cryptic asymmetry in insect spermathecae, with potential functional effects on sperm precedence in multiple-mating situations.

Cryptic asymmetry in the *D. melanogaster* spermathecae was also suggested by early studies of their developmental origins. Epper (20) located the spermathecal primordia in the early-pupal genital imaginal disc. These primordia are not found in symmetric positions across the lateral midline of the disc, but instead are aligned on the midline, with one primordium positioned more anteriorly than the other (20). This relative positioning of the spermathecal primordia was subsequently confirmed by visualization of *lz* expression at different time points during metamorphosis; *lz* is expressed in the primordia of the female accessory glands as well as the spermathecae, and is required for their development (11). Expression of *lz* at 20 h into metamorphosis shows bilaterally symmetric female accessory-gland primordia and midline-aligned spermathecal primordia (11). Based on the expression of *wingless (wg)* and *engrailed (en)* in the genital imaginal disc, Keisman et al. (21) suggested that the two spermathecal primordia occupy, respectively, an anterior and a posterior compartment of the disc. The distinct compartment origins of the two spermathecae, if confirmed, could suggest that their fates might be specified differently through development and that their differences might persist into adulthood.

Here, we first show that the morphology and physiology of the two spermathecae of *D. melanogaster* do, in fact, differ quantitatively. We then tested whether there were differences in the fundamental developmental pathways specifying the development of each spermatheca. We report lineage-tracing data using compartment-indicative markers, that show that one spermatheca forms from *en*-expressing cells (posterior compartment), whereas the other forms from *wg*-expressing cells (anterior compartment). We then show that although the developmental origin of a spermatheca does not determine its final left–right position relative to the other spermatheca, nor any gross difference in appearance or initial function between the spermathecae, there are functional differences between them in terms of sperm release dynamics. This appears to be a case of developmental system drift (22, 23) within the ontogeny of a single organism, or of phenotypic convergence (24, 25), in which different developmental programs can independently result in organs or structures with convergent form and overlapping function.

Materials and Methods

Fly Stocks and Husbandry. Fly stocks were maintained on standard glucose-yeast-agar food on a 12-h light/dark cycle at 22 °C. Unless otherwise specified, flies for crosses were kept under the same conditions, collected in single-sex vials soon after eclosion and aged 3 to 5 d before the start of the experiment. The stocks we used were 1) *en-GAL4* (Bloomington Drosophila Stock Center [BDSC] line 30564), 2) *wg-GAL4* (BDSC 4918), 3) *Send1-GAL4*, *UAS-CD63-GFP,* 4) *UAS-RFP; UAS-FLP; ubiquitous promoter-FRT-Stop-FRT-nEGFP* ("G-TRACE"; BDSC 28280), and 5) *LHm ProtB-DsRed-monomer* (referred to as *ProtB-RFP* (26); gift from the Pitnick lab). Flies carrying *UASz-jGCaMP7s-tdTomato* were generated for this study, as described below, and were crossed with *Tubulin-GAL4* (BDSC 5138) to drive expression.

Spermatheca Morphology and SSC Secretory Activity.

Fly handling. To examine the spermatheca morphology and secretory activity, unmated females and males were collected separately and aged for 3 d. Females were mated individually (1:1) or kept unmated. In all cases male-and-female pairs were observed to record mating initiation and termination times. After copulation (of at least 10 min), males were discarded and both unmated and mated females were kept singly in vials with fresh food at 25 ± 2 °C until examined.

Dissections. The female reproductive tracts of unmated and mated flies were dissected in cold Schneider's *Drosophila* media (Biological Industries). The lower reproductive tracts were isolated, cleaned of cuticle and fat-bodies, and rinsed twice to remove debris. The cleaned tract was mounted on a slide in Schneider's media.

Confocal microscopy and image processing. Spermathecae were imaged with a Leica TCS SP8 multiphoton (MP) laser scanning confocal microscope operated by LAS X software. Fluorescence was detected by using argon excitation lasers of 488 nm (for GFP), the signal of which was captured by a Hybrid detector (HyD), and of 552 nm (for nRFP), captured by a conventional photomultiplier (PMT).

SSC secretory activity. We evaluated SSC secretory activity by using a fluorescent reporter *Send1-Gal4 / UAS-CD63-GFP; +/Send1-nRFP*. To assess the GFP fluorescence intensity level, an average of 80 optical sections per spermatheca, each of 0.5 μm, were captured using the HyD with a gain of 50 or 100 and a resolution of 1024 x 1024 lines, averaging each frame three times. The actual number of optical sections per spermatheca varied, as spermathecal volume can differ between flies (see Results, below).

Measurement of spermathecal morphology and CD63-GFP fluorescence. The analysis of the CD63-GFP spermatheca characteristics was performed using Fiji [special distribution of ImageJ2 (27)]. The area, GFP mean fluorescence intensity and corrected integrated total fluorescence of different spermatheca regions were recorded by delimiting an ROI (Region of Interest) around the whole spermatheca (Total Area; At) or around the end apparatus region (Aea). To assess the activity on individual end apparatus reservoirs (EAr), ROIs were drawn around individual reservoirs, collecting 10 EAr in total per spermatheca. Background measurements were recorded per image by drawing a square ROI in an empty space of the image (containing no tissue).

Evaluation of CD63-GFP fluorescence intensity level. The corrected total fluorescence (CTF) was calculated for the At and Aea as CTF = integrated fluorescence–(area measured * background mean fluorescence). Mean GFP fluorescence intensity was measured for individual EAr and was corrected by subtracting from it the mean background fluorescence.

Measurement of Calcium Levels. *UASz-jGCaMP7s-tdTomato* was engineered by restriction digest cloning of *jGCaMP7s-tdTomato* (pGP-20XUAS-IVS-Syn21-op1-jGCaMP7s-T2A-tdTomato-p10 [Addgene plasmid # 172916; made by the GENIE Project; (28)] and *UASz1.1* (DGRC #1433) using the BamHI and KpnI sites within the *UASz1.1* vector (29), and introduced into the *attP2* docking site; injections were done by Rainbow Transgenics, followed by outcrosses to w^{1118} and

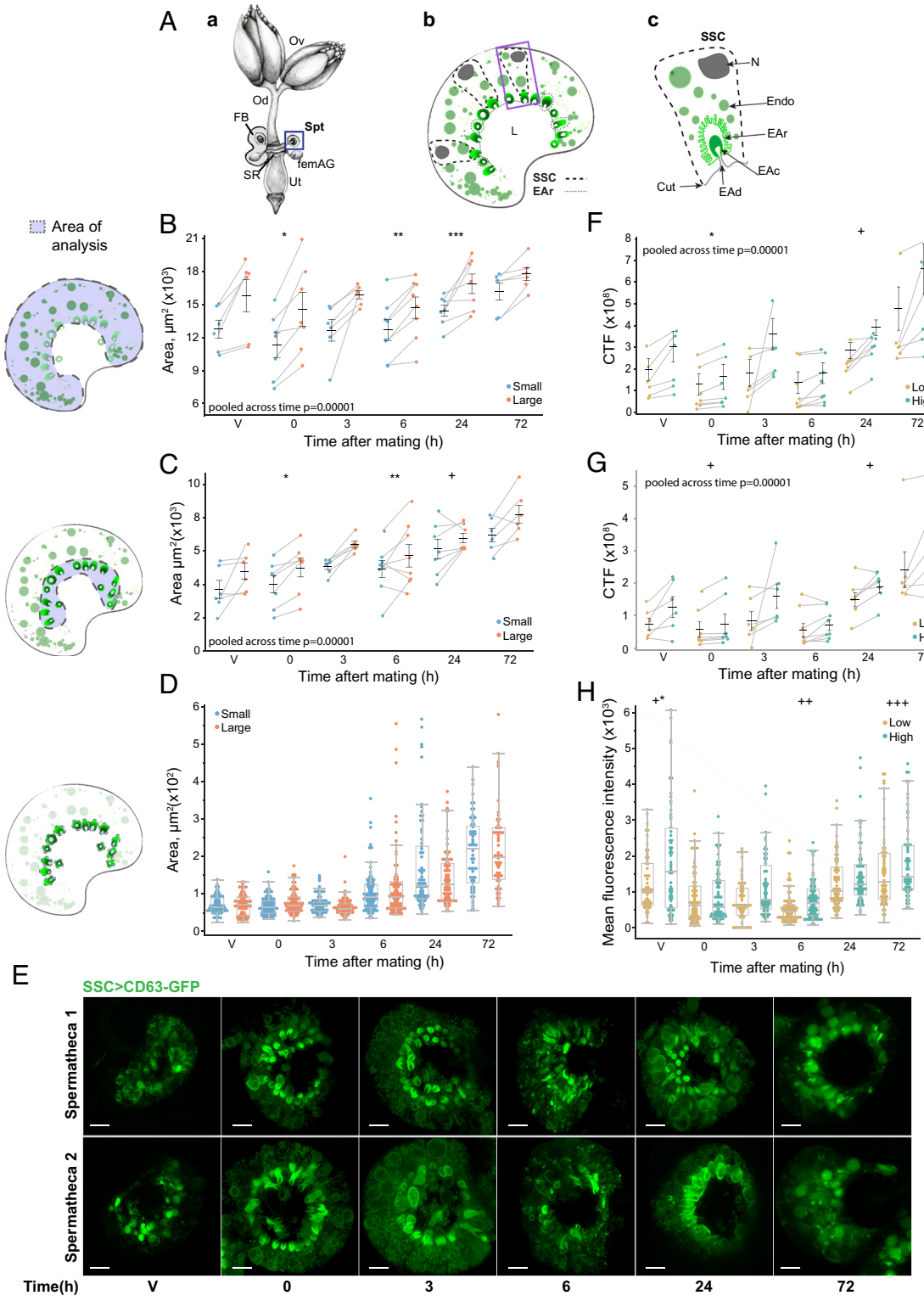

Fig. 1. Morphological and secretory activity differences within pairs of spermathecae. (*A*) (*a*) Schematic of the female reproductive tract. The reproductive tract is composed of ovaries (Ov); oviduct (Od); seminal receptacle (SR) and a pair of spermathecae (Spt), where sperm is stored; a pair of female accessory glands (femAG); and a uterus (Ut); fat body (FB) is also labeled (adapted from ref. 31). (*b*) Schematic of spermatheca (blue square in *a*) displaying the spermathecal secretory cells (SSC) radially organized around a lumen (L) where sperm is stored. (*c*) Schematic of the SSC. Each SSC displays a nucleus (N), endosomes (Endo), an end apparatus reservoir (EAr), a cuticular porous cavity (EAc) and a duct (EAd) through which secretions are secreted to the lumen; Cut = cuticle. (*B–D*) Size comparison of total spermathecal area (*B*), end apparatus region (*C*), and individual end apparatus reservoirs (*D*), as shown in the respective schematics, with "Small" and "Large" designations based on total spermathecal area. (*E*) Representative confocal images of pairs of *Send1>CD63-GFP* spermathecae at each timepoint; (Scale bar, 20 µm.) (*F–H*) Comparison of Corrected Total Fluorescence (CTF) of whole area (*F*) and end apparatus regions (*G*), with "Low" and "High" designations based on whole-area corrected total fluorescence, regardless of spermathecal size. (*H*) Comparison of mean fluorescence of individual end apparatus reservoirs between high- and low-fluorescence spermathecae. In *B*, *C*, *F*, and *G*, each line represents a single fly and symbols denote significant differences from permutation test, $*P < 0.05$ in spermathecae pairs from 6 to 8 flies; $*P = 0.037$, $**P = 0.020$, $***P = 0.036$, $+P = 0.038$. In *D* and *H*, box plots of 10 different end apparatus reservoirs from 16 to 22 flies per condition are shown, with boxes representing the 1st quartile, median, and 3rd quartile and fences extending to the farthest points that are no more than 1.5 times the difference between the 3rd and 1st quartiles. Outliers are also shown beyond the plot fences. Symbols denote significant differences from multiple comparison post hoc test, $P < 0.05$; $^{+}P = 0.002$, $^{++}P = 0.04$, $^{+++}P = 0.007$, $*P < 0.001$, $**P = 0.003$, $***P = 0.004$, $^{+*}P = 0.025$). V = unmated in panels *B–H*.

subsequent stabilization of a homozygous transgenic line. Female flies bearing *UASz-jGCaMP7s-tdTomato* were mated to *Tubulin-GAL4/TM3* males at 25 °C. Female *UASz-jGCaMP7s-tdTomato/Tubulin-GAL4* progeny were aged in the absence of males for 2 to 3 d and then mated overnight to unmated Canton-S males. Males were removed and the females were aged for ~1.5 more days, and then their reproductive tracts were dissected out and imaged. Mating was confirmed by detection of sperm in the female reproductive tracts. Female flies were briefly anesthetized on ice and reproductive tracts were dissected in 1X PBS (phosphate buffered saline) and immediately mounted on a Mattek glass bottom petri dish (P35G-1.0-14-C) in 20 uL 1X PBS with a round coverslip placed on top (Fisherbrand 12-545-82, 12CIR-1D).

Confocal microscopy, image processing, and analysis. Samples were imaged on a Zeiss LSM 880 inverted confocal microscope fitted with a C-Apochromat 40X/1.2 W Korr FCS M27 objective. GCaMP7 was detected with a 488 nm laser and tdTomato was detected with a 561 nm laser. Slices were acquired every 10 μm.

Calculation of calcium levels. For ratiometric calculations, Z-projections were generated using the "sum slices" function in Fiji/ImageJ2. Then, GCaMP7 intensity (pixels) was divided by tdTomato intensity (pixels) using Fiji's "Calculator Plus" function, which produces an image with the corresponding normalized pixel intensities. The integrated density of the spermathecae in the ratiometric images were measured by manually segmenting the spermathecae on brightfield images and applying the segmented ROI to the ratiometric images.

G-TRACE Flies and Analysis. *en>G-TRACE* and *wg>G-TRACE* females were obtained by crossing a GAL4 driver line (*en-GAL4* or *wg-GAL4*) to the G-TRACE line noted above. Reproductive tracts were dissected from live females in 1X PBS with 0.1% Triton X-100. Left and right spermathecae were determined by ascertaining where the spermathecal ducts contacted the dorsal aspect of the uterus.

Asymmetric Sperm Retention. *en>G-TRACE* and *wg>G-TRACE* females were mated to *ProtB-RFP* males in single-pair matings. Males were removed immediately after mating. Females were flash frozen in liquid nitrogen at 1 d, 4 d, and 10 d after mating. Female lower reproductive tracts were dissected in 1X PBS and imaged with an ECHO Revolve microscope to visualize EGFP signals of the spermathecae (FITC) and RFP signals of sperm heads (TxRED). Sperm heads were then manually counted using the annotation tool in the ECHO Pro app (Echo Laboratories) installed on the Revolve microscope. Sperm counting was performed without knowledge of each spermatheca's EGFP status.

Statistical Analyses.

Sperm storage. Statistical analysis was performed in R v4.4.1 with the following packages: tidyverse v2.0.0, lme4 v1.1-35.5, and emmeans v1.10.6. In analyses of sperm counts when compartmental origin was known from lineage tracing, generalized linear mixed models with Poisson link function were fitted to model the effect of each spermatheca's compartmental identity (fixed effect), time (fixed effect), their interaction (fixed effect), and female ID (random effect) on the sperm count. The marginal mean sperm count and its 95% CI for each compartmental identity was estimated within each time point using emmeans with bias adjustment for nonlinear backtransformation using the estimated SD of the female ID random effect. In analyses of sperm counts when compartmental origin was not known from lineage tracing, a G test of equal proportions of sperm in the two spermathecae was performed on each female, and the *p*-values from these tests were combined by Fisher's method to obtain an overall *p*-value. When analyzing the published data on the *spermathreecae* mutant (30), separate analyses were performed for mutant females with 3 spermathecae (testing 1/3 sperm stored in each) and mutant females with 2 spermathecae (testing 1/2 sperm stored in each). In addition, females for whom any spermatheca contained 0 sperm were excluded from the analysis because the G test cannot be computed. This exclusion is conservative because these females tended to have substantial numbers of sperm in the other spermatheca or spermathecae.

Calcium measurements. We used permutations to test whether calcium levels between the two spermathecae within a female differed more than expected by chance. Because there is a strong correlation in calcium levels between the two spermathecae in the same female, as well as high female-to-female variation in total calcium signal, we normalized each calcium level by the total calcium level per female to obtain a proportional measure of calcium level in each spermatheca. We compared the average absolute difference between the two spermathecae within a female with the same quantity calculated after permuting which calcium level belonged to which female and spermatheca. Similar permutation tests were performed to test whether calcium levels differed between unmated and mated females. The *p*-values are based on 100,000 permutations.

Spermatheca morphology and SSC secretory activity. To test whether measures of spermathecal size or secretory activity differed within females, permutations were used as described above for calcium levels. To investigate whether these measures differed across time after mating, we used the Generalized Estimating Equations procedure for correlated data (with the Gamma distribution assumption and power=1 link to explicitly model asymmetry) (SPSS V.29.0). A post-hoc pairwise comparison was used to test whether size and fluorescence intensity level differences differed across time after mating.

Results

Although Overtly Similar in Form and Function, the Two Spermathecae Have Reproducible Differences in Form, Physiology, and Function.*The two spermathecae differ in size.* A spermatheca can be roughly divided into several key regions: the central cup (or, lumen), where sperm are stored; the stalk, which connects the cup to the uterus; the body, consisting of spermathecal secretory cells (SSCs) and comprising the bulk of its volume; and the end apparatus (EA) (Fig. 1 *A*, *a*–*c*). The EA is a specialized, highly convoluted region of the SSC apical membrane, which opens directly into the cup and serves as a major endo- and exocytosis hub (9, 31). The extracellular space, adjacent to the EA membrane and in which secretory products are concentrated, is referred to as the EA reservoir. Since both endo- and exocytosis involve extensive membrane remodeling, cell surface area may be affected, and thus, may serve as a proxy for membrane transport and other cellular activities. To determine whether the spermathecae differ in size within the same fly as an inherent anatomical characteristic that might vary throughout the reproductive lifetime, we reanalyzed data from the total area, EA region, and individual EA of the spermathecal pair of unmated and mated flies at different timepoints after mating (immediate, 3 h, 6 h, 24 h, and 72 h)(31).

We observed a significant size difference between the spermathecae within a female at 0, 6, and 24 h after mating (Fig. 1*B*; $P = 0.037$, 0.020, and 0.036, respectively). Sample sizes were low at each time point, and there was no evidence of a significant change in the magnitude of the size difference across time, so we also performed the same test with all timepoints pooled together. This test showed a highly significant size difference between the spermathecae within a female, suggesting that across timepoints, there is one smaller and one larger spermatheca ($P < 0.00001$). In addition, we separately measured the area of the region the EA occupies within the spermatheca. To visualize the EA, we expressed GFP-tagged CD63, a human tetraspanin, specifically in the SSC using the *Send1* SSC-specific promoter (14, 31, 32, 33). CD63 is highly enriched within multivesicular bodies/endosomes and at the plasma membrane of the cells and extracellular vesicles membranes (31, 32, 34, 35). We found that the size of the EA region of the two spermathecae differs significantly at 0, 6, and 24 h after mating (Fig. 1*C*; $P = 0.037$, 0.020, and 0.038, respectively). Similarly to the total size, there was no evidence of a significant change in the magnitude of the EA size difference across time, and the EA size difference for all timepoints pooled together was highly significant ($P < 0.00001$). Interestingly, in both total and EA region areas, an interaction of the size with time after mating was found, where the spermathecae are larger at later times after mating compared to earlier times ($P < 0.05$). There was no association between the identity of a spermatheca as the smaller or larger one and the size of individual EA at any specific timepoint or overall (Fig. 1*D*). However, a significant effect of time after mating was observed on individual EA area (increase in individual-EA area with time after mating; $P < 0.001$).

These results show that across 72 h after mating, there is a significant difference in size between the two spermathecae. However, intriguingly, although a larger EA region corresponds with larger surface area of the entire spermatheca (Pearson's r = 0.73), the individual reservoir areas do not. This discrepancy may be explained by the enlargement of individual reservoirs starting from approximately 3 h after mating to the point at which their size no longer correlates with their respective spermathecae. Interestingly, since this enlargement does not relate to the overall spermathecae size or cell number, this suggests that it comes at the expense of the cytoplasm. Moreover, as seen previously (31), the morphology of the EA seems to change continuously between round and oval shapes (Fig. 1*E*), which affects surface area while maintaining similar volume. This phenomenon and its effect on EA reservoir function will require further investigation.

The two spermathecae differ in secretory activity. As spermathecae are major secretory organs, we examined the secretory activity of each spermatheca. As the tetraspanin CD63 is tightly associated with cellular secretion, abundant in the endosomal compartment of eukaryotic cells and on the secreting cell membrane (35), to visualize secretory/endocytic activity of the SSC we specifically expressed GFP-tagged CD63 in the SSC driven by GAL4 under the SSC-specific promoter of *Send1* (14, 31). Corrected total fluorescence (CTF) of the whole spermatheca was calculated and based on it, one spermatheca within each pair was designated as having "high" and the other "low" fluorescence status (Fig. 1*F*). We observed significant differences in fluorescence within the spermatheca pair at 0 and 24 h after mating (P = 0.037 and 0.038, respectively), but there was no evidence of a significant change in the within-female fluorescence difference across time. Hence, we analyzed the differences in fluorescence status by pooling the spermathecae from all time points and found a significant difference (P = 0.00001). We next measured CTF of the EA region (Fig. 1*G*) and found significant differences at 0 and 24 h after mating (P = 0.038 and 0.038, respectively). We also found a correlation between fluorescence of the whole spermatheca with that of the EA region (Pearson's r = 0.98), as the EA is the strongest source of fluorescence in the spermathecae. Additionally, there was no evidence of a significant change in the within-female EA fluorescence difference across time and, for all time points pooled together, the difference was highly significant (P < 0.00001). As with size, there was a significant increase in fluorescence with time after mating, both for the whole spermatheca and the EA region (P = 0.001). Finally, unlike the pattern seen for individual-EA size, the mean fluorescence of individual reservoirs (Fig. 1*H*) showed a significant association with total fluorescence at some time points (P = 0.025, 0.04, and 0.007 for unmated, 6-hr postmating, and 3-d postmating females, respectively). In all cases, no interactions were observed of the spermatheca pair fluorescence status across time. Nevertheless, differences in spermatheca pairs are not necessarily fully captured through the secretory activity measured at fixed timepoints, as secretion is a continuous and dynamic process. Taken together, these results indicate a difference in secretory activity within the pair, at least in part in conjunction with differential size, which may suggest that the two spermathecae may display differences in levels of certain functions, potentially leading to some difference in biological function (although they both store sperm).

The two spermathecae differ in calcium levels. Calcium-based signaling underlies numerous cellular processes, including secretion and sperm function. Calcium modulates various downstream pathways, including by activating a range of cytoplasmic signaling proteins (36). In reproduction, calcium signaling is essential for gamete formation and maturation, fertilization, egg activation and, in mammals, early stages of pre- and peri-implantation development (37, 38). We therefore analyzed the levels of free calcium within spermathecae, by adapting a ratiometric calcium sensor (Fig. 2*A*, *UASz-jGCaMP7s-tdTomato*). GCaMP7 is calcium-sensitive and only fluoresces when bound to free-calcium; it is fused to a tdTomato fluorophore (39), which fluoresces regardless of calcium levels and allowed us to normalize GCaMP7 fluorescence to overall expression levels of the construct in spermathecae. We validated that our construct responds to calcium by visualizing the calcium wave in activating eggs (40).

Calcium levels were compared between spermathecae by taking Z-projections of reproductive tracts of *Tubulin-GAL4>UASz-GCaMP7s-tdTomato* females. A very low background signal was detected in *UASz-GCaMP7s-tdTomato* flies lacking a *GAL4* driver (Fig. 2*D*). Pixel intensities of GCaMP7 (Fig. 2 *B′* and *C′*) projections were divided by the corresponding tdTomato (Fig. 2 *B″* and *C″*) pixels, generating a ratiometric image that represents normalized calcium levels (Fig. 2 *B‴* and *C‴*). The resulting ratiometric images emphasize regions of the spermathecae with relatively high calcium levels, or low sensor protein expression (Fig. 2, *Right* column). Interestingly, our ratiometric analysis revealed two main patterns of calcium distribution within spermathecae: concentrated on one side or fairly uniform throughout the spermatheca (*SI Appendix*, Fig. S1). These patterns were detected in both or either spermatheca, in either mated or unmated conditions (*SI Appendix*, Fig. S1).

The intensities of the spermatheca in the ratiometrically normalized images were measured (Fig. 2 *B*, *C*, *E*, and *F*) and showed a greater difference in calcium levels between the two spermathecae of the same reproductive tract than expected by chance. This was seen in both unmated and mated flies (one-sided P = 0.00043, unmated; one-sided P = 0.03985, mated). Overall calcium levels were higher in spermathecae of unmated females, with the higher-calcium and lower-calcium spermathecae each showing a significant difference between unmated and mated conditions (Fig. 2*G*, two-sided P = 0.00881 and 0.0299 for higher and lower, respectively). Interestingly, the ratio of calcium levels between the higher and lower-calcium spermatheca did not change with mating, despite the absolute change in calcium levels (Fig. 2*H*, two-sided P = 0.4091). We conclude that the two spermathecae have different levels of free calcium and that calcium levels in both spermathecae drop upon mating; however, the proportional difference in calcium between spermathecae of the same reproductive tract is maintained after mating. Depending on how calcium signals are transduced, the differences in free calcium levels between the spermathecae in a female might allow them to be physiologically, and potentially functionally, distinct.

The two spermathecae differ in sperm storage dynamics. As the results above indicated structural and physiological differences between the spermathecae, we wondered whether these differences are reflected in spermathecal function. We had previously noticed an asymmetric distribution of sperm between the spermathecae in a study focused on sperm storage and release in females with disrupted octopamine/tyramine signaling after mating with two genetically distinct males (41). Here, we reanalyzed the results and designated each spermatheca as either "major" or "minor" based on which contained more sperm in each female. In a series of parallel experiments with flies of different genetic constitution, we found that over time as sperm were released from the spermathecae and the total spermathecal sperm count decreased, the level of asymmetry increased (*SI Appendix*, Fig. S2 *A–C*). This finding suggests that asymmetric sperm retention is common across lab strains of *D. melanogaster* females. The increase in asymmetry of retained sperm numbers could be caused by equal recruitment into storage followed by differential depletion, by differential

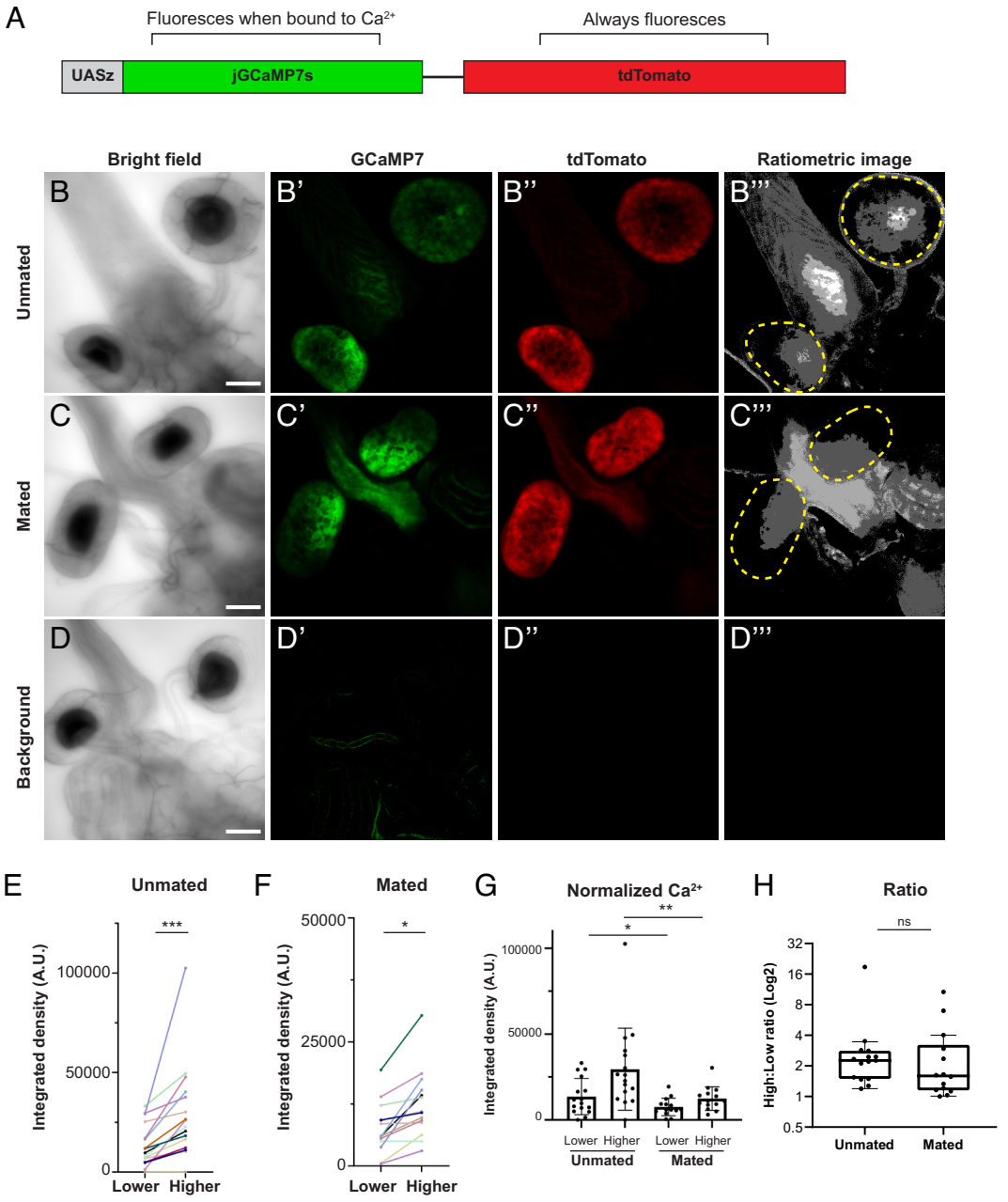

Fig. 2. Calcium levels differ between spermathecae. (*A*) Schematic diagram of the *UASz-jGCaMP7s-tdTomato* construct. (*B–D‴*) Summed z-projections of spermathecae from *Tubulin-GAL4>UASz-GCaMP7s-tdTomato* unmated (*B* and *B‴*) or mated (*C* and *C‴*), or *UASz-GCaMP7s-tdTomato/TM3* unmated control (*D* and *D‴*) in brightfield (*B–D*), green (*B′–D′*, GCaMP7), or red (*B″–D″*, tdTomato) channels. Ratiometric images (*B‴–D‴*) were generated by dividing GCaMP7 fluorescence integrated density by tdTomato integrated density. Yellow dashed lines mark the measured regions; boundaries were drawn manually using the corresponding brightfield images. The display range of ratiometric images was uniformly adjusted to increase visibility of ratiometric signal; all measurements were performed on raw ratiometric images. (*E*) Quantification of (*B‴*), with "Lower" and "Higher" designations for the two spermathecae within a female based on the ratiometric data. (*F*) Quantification of (*C‴*), with "Lower" and "Higher" designations as in (*E*). (*G*) Calcium levels were higher overall in spermathecae from unmated females compared to mated. (*H*) The ratio (shown on a log2 scale with box plots as in Fig. 1 *D* and *H*) between higher:lower calcium spermathecae did not change between spermathecae of unmated and mated female flies. Unmated = 16 reproductive tracts, mated = 14 reproductive tracts, from three biological replicates per condition. In *E–H*, symbols denote significant differences: **P* < 0.05; ***P* < 0.01; ****P* < 0.001; *P*-values are derived from permutation tests, as described in *Calcium measurements*. (Scale bar, 50 μm.)

recruitment followed by equal depletion, or both retention and depletion could be asymmetric.

The Two Spermathecae Derive from Different Compartments, and this Underlies the Difference in Their Sperm Retention Dynamics. ***The two spermathecae derive from different compartments.*** The differences between the spermathecae suggested that they might reflect different developmental origins, despite both deriving from the genital disc. To test whether the inference of different compartment origins for the two spermathecae was correct, we visualized the cell lineages of these compartments in the adult female reproductive tract using the G-TRACE system (Fig. 3*A*), which expresses GFP in all cells descending from any cell in which a GAL4 driver had been expressed at a sufficient level to activate expression of FLP recombinase, which in turn excises a transcription-termination sequence to enable constitutive expression of a GFP reporter (42).

We found that a *wg* GAL4 driver, in combination with the G-TRACE system (hereafter *wg>G-TRACE*), consistently showed GFP expression in exactly one spermatheca per female (Fig. 3 *B*

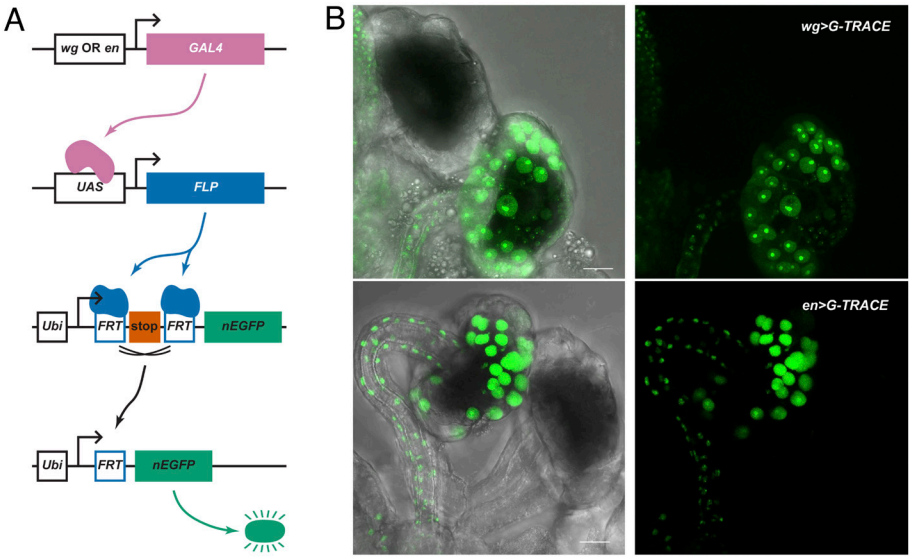

Fig. 3. The spermathecae derive from different developmental compartments. G-TRACE was used to mark descendants of *en*-expressing or *wg*-expressing cells. In each case, exactly one spermatheca per female expresses the G-TRACE lineage marker, GFP. (*A*) G-TRACE uses an *en-GAL4* or *wg-GAL4* driver to produce GAL4 protein (pink), which binds to its corresponding *UAS* sequence to induce expression of FLP recombinase (blue) in the *en*-expressing or *wg*-expressing cells. FLP in turn causes recombination between *FRT* sites flanking a transcription termination (stop) sequence, excising that sequence (orange) and thereby allowing expression of a nuclear-localized EGFP (green) in the cell in which recombination occurs and all of its descendant cells. G-TRACE flies also contain a *UAS-RFP* reporter that marks cells currently expressing GAL4, but this signal was not used in these experiments (because the drivers are not expressed in adult spermathecae) and is not shown. (*B*) The two spermathecae of a *wg>G-TRACE* adult female (*Top*) and an *en>G-TRACE* adult female (*Bottom*). For each, the GFP channel (*Right*) is shown overlaid on a brightfield image (*Left*), and exactly one spermatheca expresses GFP.

Top), presumably the anterior one. Likewise, an *en* GAL4 driver, in combination with the G-TRACE system (*en>G-TRACE*), consistently showed GFP expression in exactly one spermatheca per female (Fig. 3 *B Bottom*), presumably the posterior one.

We next tested whether the presumptive posteriorly derived spermatheca ends up preferentially on the left or right side of the adult female. We scored the side on which the presumptive posteriorly derived spermatheca was found in 145 *en>G-TRACE* females (as determined by expression of GFP) and in 145 *wg>G-TRACE* females (as determined by lack of expression of GFP). Of these 290 spermathecae, 152 were found on the left and 138 were found on the right, indicating that there is no preferential direction of rotation of the anterior and posterior primordia to their final lateral positions ($P = 0.45$, binomial test).

The spermathecae from different compartments have different sperm-retention dynamics. Given that the two spermathecae have distinct developmental origins, we asked whether they were functionally different with respect to sperm storage. Using the G-TRACE system to mark the *en*-derived or *wg*-derived spermatheca in separate experiments, we mated *en>G-TRACE* and *wg>G-TRACE* females to *ProtB-RFP* males to facilitate sperm counting. In order to examine both short and long-term sperm storage, we used three time points after mating: 1 d, 4 d, and 10 d.

For the *en>G-TRACE* experiment, at 1 and 4 d after mating, the GFP^- and GFP^+ spermathecae had statistically indistinguishable sperm counts (Fig. 4*A*), suggesting that initial sperm storage and release did not differ by spermatheca identity. The same result was seen for the *wg>G-TRACE* experiment at 1 and 4 d after mating (Fig. 4*B*). However, by 10 d after mating, the GFP^+ spermatheca in the *en>G-TRACE* females retained more sperm than the GFP^- spermatheca (Fig. 4*A*; 10 d comparison $P < 10^{-8}$). Consistent with compartmental identity determining the difference in sperm storage, the opposite trend was observed in the *wg>G-TRACE* females, with their GFP^- spermatheca retaining more sperm than the GFP^+ spermatheca (Fig. 4*B*; 10 d comparison $P < 0.0001$). Because the *en>G-TRACE* and *wg>G-TRACE* experiment complement each other, we combined the results from both experiments for further analysis. The combined results corroborated the separate analyses that the *en*-derived (posterior) spermatheca retained more sperm than the *wg*-derived (anterior) spermatheca at 10 d after mating; in addition, a small, statistically significant difference is apparent at 4 d after mating (Fig. 4*C*; 10 d comparison $P < 10^{-8}$, 4 d comparison $P = 0.013$). The pattern of increasing asymmetry is apparent when the proportion of sperm in the posterior-derived spermatheca is plotted across the three time points (Fig. 4*D*). When we removed the spermathecae's *en* and *wg* labels from the results of the *G-TRACE* experiment, and instead simply applied the major/minor designation based on sperm count, we found similar levels of asymmetry as we had observed with the other strains, previously (*SI Appendix*, Fig. S2*D*). Moreover, there is strong statistical evidence that the two spermathecae do not contain equal proportions of sperm, as tested by combining *p*-values from tests of equal proportions from individual females (combined $P < 10^{-8}$ at each time point). Because this departure from equal proportions is seen at each time point, whereas a difference in anterior-derived spermatheca vs. posterior-derived spermatheca sperm count is not seen at day 1 after mating, it is possible that there are two aspects of asymmetry at play: a bias toward retaining sperm in the posterior-derived spermatheca, as well as a compartment-independent propensity to store sperm unequally in the two spermathecae. This latter conclusion is supported by our analysis of recently published data from female *spermathreecae* mutants (30), which are very likely to develop with three rather than two spermathecae. We find that, at each of five different time points after mating (day 1, 5, 10, 15, or 20), and in mutant females with two or three spermathecae, there is strong statistical evidence of unequal proportions of sperm in the spermathecae of the same female ($P < 10^{-8}$ in each case).

Discussion

We have shown that *D. melanogaster* spermathecae show asymmetries in form and function, including significant differences in size, secretory activity, calcium levels, and sperm retention.

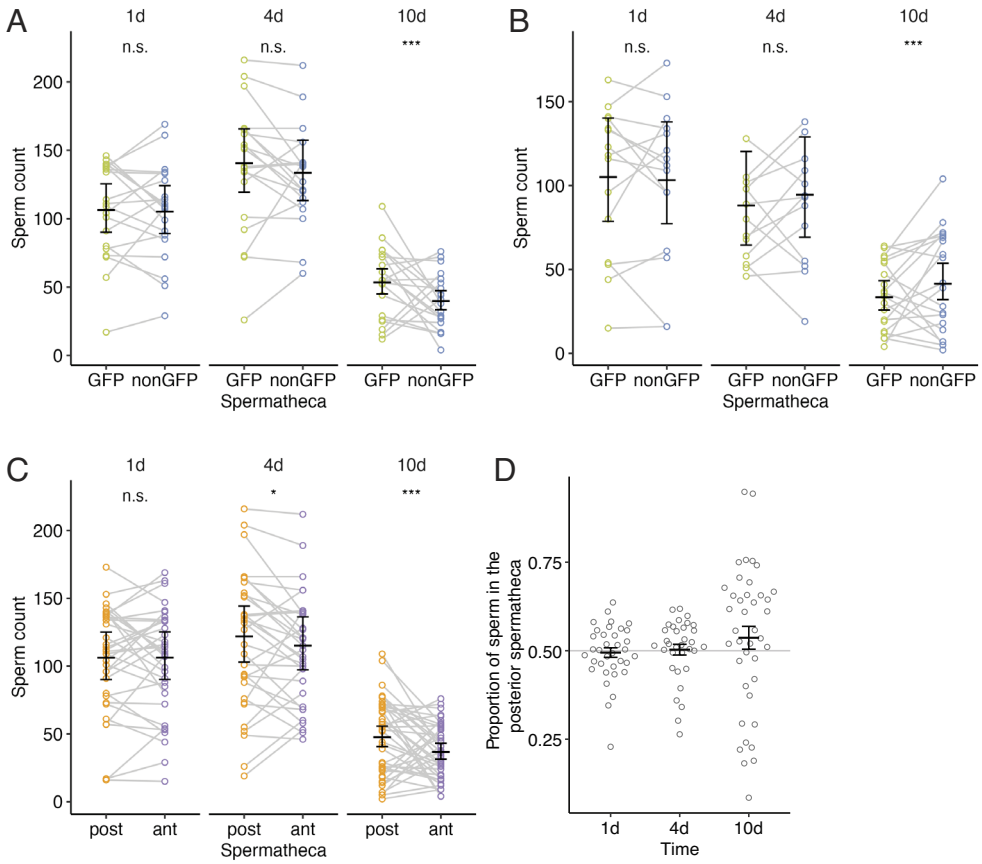

Fig. 4. The *en* spermatheca retains more sperm than the *wg* spermatheca at 10 d after mating. *en>G-TRACE* females and *wg>G-TRACE* females were mated to *ProtB-RFP* males and sperm stored in each spermatheca were counted at 1 d, 4 d, and 10 d after mating. (*A*) Number of sperm in the GFP (green) and non-GFP (blue) spermatheca of *en>G-TRACE* females (n = 20 females for each timepoint). (*B*) Number of sperm in the GFP (green) and non-GFP (blue) spermatheca of *wg>G-TRACE* females (n = 15, 13, and 20 females for the 1 d, 4 d, and 10 d timepoints, respectively). (*C* and *D*) Results from *en>G-TRACE* and *wg>G-TRACE* females were combined. (*C*) Number of sperm in the posterior (orange) and anterior (purple) spermatheca. (*D*) Proportion of spermathecal sperm found in the posterior-derived spermatheca. The horizontal gray line at 0.50 represents equal proportions. In (*A*–*C*) lines connect spermathecae in the same female. n.s. not significant; $*P < 0.05$, $***P < 0.001$. Error bars show mean and 95% CI.

Although asymmetries have been observed in the spermathecae of other insects [e.g. mosquitoes (15), yellow dung flies (16), and Mediterranean fruit flies (17)], *D. melanogaster* presents a uniquely powerful system for integrating developmental, physiological, behavioral, and population-level investigations to understand the causes and reproductive consequences of asymmetry.

When otherwise bilaterally symmetric organs have distinct functions, there are several possible, nonmutually exclusive explanations. One possibility is adaptive evolution of the divergence, for example natural selection for division of functions. *D. melanogaster* has long been understood to have division of functions between two different types of sperm-storage organs—the spermathecae, which are used for long-term storage and have high secretory activity, and the seminal receptacle, which stores the majority of the sperm and is used for short-term storage (43). Divergence between the two spermathecae could add a layer of specialization on top of the spermathecae/seminal receptacle division, for example by contributing to cryptic female choice (44). Remating causes most of the sperm in the seminal receptacle to be ejected and replaced by the second male′s sperm, whereas the spermathecae retain a larger portion of the first male′s sperm, potentially allowing the female to control the sire of her progeny (26). Inherent differences between the two spermathecae might allow differential recruitment or retention of sperm, and thereby greater control of paternity. The existence of a size difference between the two spermathecae at the time of mating supports the idea that differences are inherent, rather than a result of chance variation in the number of sperm stored. The difference in sperm counts between the anterior and posterior spermathecae supports the idea that differences are inherent as well. Thus, given the differences we observed in morphology and calcium levels between the spermathecae, it is possible that they have differences in function, for example one spermatheca might play a bigger role in storing sperm and the other in signaling.

A second possibility for divergence from perfect bilateral symmetry is that symmetry, to the extent that it exists, is imposed over a developmental process that is not symmetric. The ancestral number and form of the spermatheca is not known (45), which leaves several possibilities for the evolutionary origin(s) of spermathecal asymmetry in insects. One intriguing possibility to consider is that directional asymmetry arises from a state of "antisymmetry," wherein the existence of a difference between members of a pair is initially favored, followed by the evolution of regulatory mechanisms that impart consistently distinct identities (46). Investigations of the compartmentally distinct origins of the spermathecae in other insects could reveal whether the asymmetry seen in *D. melanogaster* is the product of such an evolutionary transition. Such investigations could also help contextualize how similarities between the two spermathecae arise despite differences in development. The ability of En and Wg to control cell-fate decisions suggests that asymmetry between the two spermathecae is inherent but can be overridden in numerous respects by other regulators, possibly including Lz and Hr39, to result in a relatively similar outcome. In other words, similarities in function between

the two spermathecae could be a case of phenotypic convergence of initially distinct developmental processes (24, 25).

It is possible that the differences that remain between the anterior-derived and posterior-derived spermathecae are advantageous, with natural selection preserving these differences against complete phenotypic convergence. However, until such an evolutionary advantage is shown, it is also possible that the remaining differences between the spermathecae are not adaptive. Instead, these differences could be a result of developmental system drift (22, 23) within the ontogeny of a single organism. In other words, the compartmental-origin difference might create different regulatory environments in the two spermathecae that allow other molecular differences to accrue neutrally, without impacting physiological function in a deleterious way. From this perspective, the observed levels of quantitative difference in spermathecal size, secretory activity, calcium levels, and even sperm retention dynamics, might not impact the reproductive fitness of the organism.

To distinguish among these possibilities, and to further establish *D. melanogaster* as a model for the mechanisms and consequences of spermathecal asymmetry in other insect species, it will be important to learn more about the developmental and functional differences between the spermathecae. One important avenue to explore will be the innervation of the spermathecae, as neural control of their musculature and physiology plays key roles in sperm storage (47). Considering the origins of the spermathecae in separate anterior and posterior compartments of the genital imaginal disc, it is notable that a pair of neurons that innervate one spermatheca each have cell bodies in the ventral nerve cord that are located anterior and posterior relative to each other, rather than left and right (48). This parallel organization could aid in understanding how asymmetric structures are controlled independently by the nervous system.

Greater understanding of the developmental and functional differences between the spermathecae might also be gained by studying two recently described mutants of *D. melanogaster*, in which females very frequently develop with three spermathecae instead of two (30, 49). Indeed, one of these is a mutation in *en* (49), further study of which might reveal how *en* expression impacts spermathecal development and function. The other mutant is in a previously uncharacterized gene, now named *spermathreecae* (30). In *spermathreecae*-mutant females, two out of the three spermathecae tend to share part of a spermathecal duct, implying a shared developmental origin. If this duct sharing were consistently associated with the *wg*-expressing or *en*-expressing spermathecal primordium, it could shed additional light on the relevant developmental process. This association could be tested by combining the *spermathreecae* mutation (30) with the G-TRACE system (42). It could also be fruitful to revisit experiments on fecundity and sperm competition in G-TRACE-marked flies, to potentially reveal greater functional consequences of the distinct identities of the two spermathecae.

Our results also suggest that it would be promising to study the developmental origins of spermathecae in other insects that show obvious asymmetry in these organs. For example, do the doublet vs. singlet spermathecae of the yellow dung fly (or the medial and lateral spermathecae of mosquitoes) arise from different genital-disc compartments? It would also be interesting to test whether the two spermathecae of the Mediterranean fruit fly (17) derive respectively from *wg*-expressing and *en*-expressing compartments, and if so whether the unequal storage that is reported correlates with compartmental identity. Such investigations could help advance understanding (and potential manipulation) of fertility in agriculturally and medically important species.

Data, Materials, and Software Availability. All study data are included in the article and/or *SI Appendix*.

ACKNOWLEDGMENTS. We thank R01HD059060 to M.F.W. and A.G.C., R37HD038921 to M.F.W., R35GM148344 to M.L.S., ISF-2041/17 and 2470/21 to Y. Heifetz., and a Cornell Mann Award to J.M.T. for funding. Stocks obtained from the Bloomington Drosophila Stock Center (NIH P40OD018537) were used in this study, except for the protamine-GFP flies, for which we thank Scott Pitnick. Thanks to Sean Karott, Stephanie Lauer, Tyler Douglas, Vanessa Lu, and Daniel McNelis for help with pilot experiments on cell-lineage tracing. We also thank Amir Hefetz for his help with statistics.

Author affiliations: [a]Department of Molecular Biology and Genetics, Cornell University, Ithaca, NY 14853; [b]Center for Genomics and Systems Biology, Department of Biology, New York University, New York, NY 10003; and [c]Department of Entomology, The Hebrew University of Jerusalem, Rehovot 7610001, Israel

1. R. M. Soriano, D. Penfold, S. W. Leslie, *Anatomy, Abdomen and Pelvis: Kidneys* [StatPearls, 2025].
2. M. Friedman, The evolutionary origin of flatfish asymmetry. *Nature* **454**, 209–212 (2008).
3. F. Halle, M. Gahr, A. W. Pieneman, M. Kreutzer, Recovery of song preferences after excitotoxic HVC lesion in female canaries. *J. Neurobiol.* **52**, 1–13 (2002).
4. S. Takeda, M. Murai, Asymmetry in male fiddler crabs is related to the basic pattern of claw-waving display. *Biol. Bull.* **184**, 203–208 (1993).
5. J. Gordon Betts, *Anatomy & Physiology* (OpenStax College, Rice University, 2013).
6. R. Shine, M. M. Olsson, M. P. LeMaster, I. T. Moore, R. T. Mason, Are snakes right-handed?: Asymmetry in hemipenis size and usage in gartersnakes. *Behav. Ecol.* **11**, 411–415 (2000).
7. S. Guioli, D. Zhao, S. Nandi, M. Clinton, R. Lovell-Badge, Oestrogen in the chick embryo can induce chromosomally male ZZ left gonad epithelial cells to form an ovarian cortex that can support oogenesis. *Development* **147**, dev181693 (2020).
8. I. Jarvela, S. Nuojua-Huttunen, H. Martikainen, Ovulation side and cycle fecundity: A retrospective analysis of frozen/thawed embryo transfer cycles. *Hum. Reprod.* **15**, 1247–1249 (2000).
9. M. L. Mayhew, D. J. Merritt, The morphogenesis of spermathecae and spermathecal glands in *Drosophila melanogaster*. *Arthropod Struct. Dev.* **42**, 385–393 (2013).
10. R. C. Anderson, A study of the factors affecting fertility of lozenge females of *Drosophila melanogaster*. *Genetics* **30**, 280–296 (1945).
11. S. S. Chatterjee, L. D. Uppendahl, M. A. Chowdhury, P. L. Ip, M. L. Siegal, The female-specific doublesex isoform regulates pleiotropic transcription factors to pattern genital development in *Drosophila*. *Development* **138**, 1099–1109 (2011).
12. A. K. Allen, A. C. Spradling, The Sf1-related nuclear hormone receptor Hr39 regulates *Drosophila* female reproductive tract development and function. *Development* **135**, 311–321 (2008).
13. W. Shen, J. Sun, Dynamic notch signaling specifies each cell fate in *Drosophila* spermathecal lineage. *G3 Genes|Genomes|Genetics* **7**, 1417–1427 (2017).
14. S. L. Schnakenberg, W. R. Matias, M. L. Siegal, Sperm-storage defects and live birth in *Drosophila* females lacking spermathecal secretory cells. *PLoS Biol.* **9**, e1001192 (2011).
15. M. C. Carrasquilla, L. P. Lounibos, N. A. Honorio, S. Murr, Spermathecal filling in *Aedes aegypti* and *Aedes albopictus*: Effects of female and male body sizes and species. *J. Med. Entomol.* **56**, 334–340 (2019).
16. M. Otronen, P. Reguera, P. I. Ward, Sperm storage in the yellow dung fly *Scathophaga stercoraria*: Identifying the sperm of competing males in separate female spermathecae. *Ethology* **103**, 844–854 (1997).
17. P. W. Taylor, R. Kaspi, B. Yuval, Copula duration and sperm storage in Mediterranean fruit flies from a wild population. *Physiol. Entomol.* **25**, 94–99 (2000).
18. K. Iida, D. R. Cavener, Glucose dehydrogenase is required for normal sperm storage and utilization in female *Drosophila melanogaster*. *J. Exp. Biol.* **207**, 675–681 (2004).
19. A. C. P. Gandara, D. Drummond-Barbosa, Chronic exposure to warm temperature causes low sperm abundance and quality in *Drosophila melanogaster*. *Sci. Rep.* **13**, 12331 (2023).
20. F. Epper, The evagination of the genital imaginal discs of *Drosophila melanogaster*: I. Morphogenesis of the female genital disc. *Wilhelm Roux Arch. Dev. Biol.* **192**, 275–279 (1983).
21. E. L. Keisman, A. E. Christiansen, B. S. Baker, The sex determination gene doublesex regulates the A/P organizer to direct sex-specific patterns of growth in the *Drosophila* genital imaginal disc. *Dev. Cell* **1**, 215–225 (2001).
22. K. M. Weiss, S. M. Fullerton, Phenogenetic drift and the evolution of genotype-phenotype relationships. *Theor. Popul. Biol.* **57**, 187–195 (2000).
23. J. R. True, E. S. Haag, Developmental system drift and flexibility in evolutionary trajectories. *Evol. Dev.* **3**, 109–119 (2001).
24. P. Tschopp, C. J. Tabin, Deep homology in the age of next-generation sequencing. *Philos. Trans. R. Soc. Lond. B. Biol. Sci.* **372**, 20150475 (2017).
25. N. Konstantinides *et al.*, Phenotypic convergence: Distinct transcription factors regulate common terminal features. *Cell* **174**, 622–635 e613 (2018).
26. M. K. Manier *et al.*, Resolving mechanisms of competitive fertilization success in *Drosophila melanogaster*. *Science* **328**, 354–357 (2010).
27. J. Schindelin *et al.*, Fiji: An open-source platform for biological-image analysis. *Nat. Methods* **9**, 676–682 (2012).
28. H. Dana *et al.*, High-performance calcium sensors for imaging activity in neuronal populations and microcompartments. *Nat. Methods* **16**, 649–657 (2019).

29. S. Z. DeLuca, A. C. Spradling, Efficient expression of genes in the *Drosophila* germline using a UAS promoter free of interference by Hsp70 piRNAs. *Genetics* **209**, 381–387 (2018).
30. A. Dhillon, T. Chowdhury, Y. E. Morbey, A. J. Moehring, Reproductive consequences of an extra long-term sperm storage organ. *BMC Evol. Biol.* **20**, 159 (2020).
31. J. A. Sanchez-Lopez *et al.*, Male–female communication enhances release of extracellular vesicles leading to high fertility in *Drosophila*. *Commun. Biol.* **5**, 815 (2022).
32. L. Corrigan *et al.*, BMP-regulated exosomes from *Drosophila* male reproductive glands reprogram female behavior. *J. Cell Biol.* **206**, 671–688 (2014).
33. J. C. Gross, V. Chaudhary, K. Bartscherer, M. Boutros, Active Wnt proteins are secreted on exosomes. *Nat. Cell Biol.* **14**, 1036–1045 (2012).
34. D. Panakova, H. Sprong, E. Marois, C. Thiele, S. Eaton, Lipoprotein particles are required for Hedgehog and Wingless signalling. *Nature* **435**, 58–65 (2005).
35. T. Kobayashi *et al.*, The tetraspanin CD63/lamp3 cycles between endocytic and secretory compartments in human endothelial cells. *Mol. Biol. Cell* **11**, 1829–1843 (2000).
36. M. J. Berridge, P. Lipp, M. D. Bootman, The versatility and universality of calcium signalling. *Nat. Rev. Mol. Cell Biol.* **1**, 11–21 (2000).
37. D. R. Armant, Intracellular Ca2+ signaling and preimplantation development. *Adv. Exp. Med. Biol.* **843**, 151–171 (2015).
38. J. Kashir, R. Deguchi, C. Jones, K. Coward, S. A. Stricker, Comparative biology of sperm factors and fertilization-induced calcium signals across the animal kingdom. *Mol. Reproduct. Dev.* **80**, 787–815 (2013).
39. T. X. Dong *et al.*, T-cell calcium dynamics visualized in a ratiometric tdTomato-GCaMP6f transgenic reporter mouse. *eLife* **6**, e32417 (2017).
40. T. Kaneuchi *et al.*, Calcium waves occur as *Drosophila* oocytes activate. *Proc. Natl. Acad. Sc. U.S.A.* **112**, 791–796 (2015).
41. D. S. Chen, A. G. Clark, M. F. Wolfner,Octopaminergic/tyraminergic *Tdc2* neurons regulate biased sperm usage in female *Drosophila melanogaster*. *Genetics* 221, iyac096 (2022).
42. C. J. Evans *et al.*, G-TRACE: Rapid Gal4-based cell lineage analysis in *Drosophila*. *Nat. Methods* **6**, 603–605 (2009).
43. S. Pitnick, G. S. Spicer, T. A. Markow, How long is a giant sperm?. *Nature* **375**, 109 (1995).
44. W. G. Eberhard, *Female Control: Sexual Selection by Cryptic Female Choice* (Princeton Univ. Press, Princeton, NJ, 1996), p. 472.
45. T. V. Pascini, G. F. Martins, The insect spermatheca: An overview. *Zoology (Jena)* **121**, 56–71 (2017).
46. A. J. Carter, E. Osborne, D. Houle, Heritability of directional asymmetry in *Drosophila melanogaster*. *Int. J. Evol. Biol.* **13**, 759159 (2010).
47. M. A. White, D. S. Chen, M. F. Wolfner, She's got nerve: roles of octopamine in insect female reproduction. *J. Neurogenet.* **35**, 132–153 (2021).
48. E. W. Rohrbach *et al.*, Heterogeneity in the projections and excitability of tyraminergic/octopaminergic neurons that innervate the *Drosophila* reproductive tract. *Front. Mol. Neurosci.* **17**, 1374896 (2024).
49. Y. Kato *et al.*, A new allele of engrailed, en(NK14), causes supernumerary spermathecae in *Drosophila melanogaster*. *Genes Genet. Syst.* **96**, 259–269 (2022).